

XMM-NEWTON, SWIFT AND ROSAT OBSERVATIONS OF LBQS 0102-2713

TH. BOLLER¹, P. SCHADY¹ AND T. HEFTRICH²¹Max-Planck-Institut für extraterrestrische Physik Garching, PSF 1312, 85741 Garching, Germany²GSF Helmholtzzentrum für Schwerionenforschung GmbH, Planckstr. 1, 64291 Darmstadt, Germany*Draft version September 3, 2018*

ABSTRACT

We have analyzed the first XMM-Newton, Swift and archival ROSAT PSPC observations of the quasar LBQS 0102-2713. The object was selected from the ROSAT archive as being notable due to the steep soft X-ray photon index and due to the UV brightness based on HST and optical spectroscopic observations. The first XMM-Newton observations carried out in December 2009 and the first Swift observations from 2010 have confirmed the steepness of the soft X-ray photon index, which ranges between 3.35 and 4.41 for the different XMM-Newton and ROSAT detectors, the UV brightness of the source and the absence of significant absorption by neutral hydrogen. The new data allow a combined spectral fitting to the Swift UVOT and the XMM-Newton/ROSAT data which results in a huge luminosity of $(6.2 \pm 0.2) \times 10^{47}$ erg s⁻¹ and α_{ox} values ranging between (-1.87 ± 0.11) and (-2.11 ± 0.12) . The nature of the soft X-ray emission can be explained as local comptonized emission of the UV disc photons in the pseudo-Newtonian potential. The black hole mass is estimated from the Mg II line and translates into an Eddington ratio of $L/L_{\text{edd}} = 18^{+33}_{-12}$. For the dimensionless electron temperature of the plasma cloud $\theta = kT_e/m_e c^2$ we derive an upper limit of about 10 keV.

Subject headings: AGN: general – X-rays: galaxies – galaxies: active – Quasars: individual LBQS 0102-2713

1. INTRODUCTION

LBQS 0102-2713 is a Narrow-Line Quasar at a redshift of $z = 0.780 \pm 0.005$ with a B magnitude of 17.52 ± 0.15 (Hewett et al. 1995). The object was selected from the catalogue of ROSAT pointed observations as being notable and important due to its steep photon index for a quasar (Boller et al. 2009). The photon index obtained from a power law fit was $\Gamma = (6.0 \pm 1.3)$ for an N_{H} value of $(4.8 \pm 1.5) \times 10^{20}$ cm⁻². The photon index remained steep at about 3.5 when the N_{H} value was fixed to the Galactic value of 1.2×10^{20} cm⁻² (Dickey and Lockman, 1990). The α_{ox} was steep with a value of about -2.3, comparable to the steepest values detected in BAL quasars. However, the maximum intrinsic absorption was at least a factor of about 20 lower compared to BAL quasars.

The Mg II line at 2800 Å rest frame has a FWHM of about 2200 km s⁻¹ (c.f. Fig. 4 of Boller et al. 2009). This value is very close to the somewhat arbitrary line between Narrow-Line Seyfert 1 Galaxies (NLS1s) and broad line Seyfert galaxies of 2000 km s⁻¹ following the definition of Osterbrock & Pogge (1985). As the 2000 km s⁻¹ arbitrary line is luminosity dependent (Shemmer et al. 2008), LBQS 0102-2713 can be considered as a luminous NLS1. In addition there is strong UV Fe II multiplet emission between about 2200 and 2500 Å in the rest frame. All this is typical for NLS1s (c.f. Trümper & Hasinger 2008).

There are no significant indications that the object is intrinsically X-ray weak, in contrast to the argument used for PHL 1811 by Leighly et al. (2007). In the case of an intrinsically weak X-ray source one expects weak low ionization or semiforbidden UV lines. The rest-frame EW values of LBQS 0102-2713 for the blend of Ly β and the

O VI lines, and the Ly α and the N V lines are about 12 and 50 Å, respectively when comparing these values with quasar composites the source appears not to be intrinsically X-ray weak. For the Ly β plus O VI lines Brotherton et al. (2001) give an EW value of 11 Å in the rest frame and for the blend of Ly α and N V a value of 87 Å. Similar values can be found in the quasar composites of Vanden Berk et al. (2001) and Zheng et al. (1997).

In this paper we analyse the first XMM-Newton and Swift observation of the source and give tighter constraints on the important α_{ox} and soft X-ray photon index values, the black hole mass, UV-soft X-ray luminosity and the Eddington ratio.

2. X-RAY, UV OBSERVATIONS AND DATA ANALYSIS

LBQS 0102-2713 was observed for the first time with XMM-Newton during revolution 1829 in December 2009 for 22218 seconds. The Swift XRT and UVOT observation were taken in August 2010 with total exposure times of 5079 seconds for the UVOT and 5151 seconds for the XRT measurements. ROSAT PSPC observations are available for three pointings in January, June and December 1992 with 6157, 2191, and 6724 second exposures, respectively. In Table 1 we list the count rates and exposure times for the individual detectors. The unobscured flux and luminosity is derived in the Section 4.

The XMM-Newton observations were processed using SAS 10.0.0 (xmmas_20100423_180110.0.0). The spectra and response values have been calculated by using the latest pn and MOS chains. We have fitted the XMM-Newton spectra in the energy range between 0.3 and 2.0 keV where the source is not background dominated. We note that we have carefully ignored high background flaring events and find that more than 90 per cent of MOS

TABLE 1
COUNT RATES AND EXPOSURE TIMES FOR THE XMM-NEWTON
EPIC PN, MOS1, MOS2 AND THE SWIFT UVOT DETECTORS.

Instrument	count rate [counts s ⁻¹]	exposure time [ks]
pn	$(1.20 \pm 0.01) \times 10^{-1}$	15.150
M1	$(2.26 \pm 0.13) \times 10^{-2}$	20.260
M2	$(2.10 \pm 0.12) \times 10^{-2}$	20.780
ROSAT	$(4.80 \pm 0.29) \times 10^{-2}$	12.540
Swift v	1.70 ± 0.06	1.073
Swift u	5.30 ± 0.15	1.017
Swift uvw1	3.10 ± 0.08	1.218
Swift uvw2	3.00 ± 0.08	1.245

observations and more than 65 per cent of the pn observations could be used in the subsequent data analysis. The spectra are binned using the *grppha* command. Each bin contains at least 30 counts. The Swift data were processed via the standard data analysis procedures. The data analysis of the archival ROSAT observation are described in detail in Boller et al. (2009) and are based on the *xselect* command interface. The spectral fitting results are obtained using *XSPEC*, version 12.4.0 (Arnaud et al. 1996).

3. XMM-NEWTON, ROSAT AND SWIFT XRT X-RAY DATA

3.1. LBQS 0102-2713 as a steep soft X-ray spectrum quasar

The ROSAT and XMM-Newton spectra have been fitted simultaneously, but allowing the respective values for the photon indices and normalizations to vary, given the large time difference between the observations. Spectral fitting was performed up to 2 keV, since above that energy the emission is background dominated. A simple power law model with neutral absorption results in a statistically acceptable fit. An N_H value is obtained from the ROSAT data of $2.85 \times 10^{20} \text{ cm}^{-2}$, with $\Delta\chi^2 = 2.71$ confidence levels ranging between $(2.2 \text{ and } 3.6) \times 10^{20} \text{ cm}^{-2}$, indicating that absorption above the Galactic value is required. In the simultaneous fit to the XMM-Newton and ROSAT data the N_H value was fixed to the value obtained from ROSAT observations. At the $\Delta\chi^2 = 2.71$ confidence level the photon indices range between 3.35 and 4.41. The Swift XRT data exhibit the lowest count rate statistics with $(4.0 \pm 0.9) 10^{-3} \text{ counts s}^{-1}$ and are not included into the joint fit as the power law and normalization values remain unconstrained. The normalization values obtained from the XMM-Newton and ROSAT data indicate no significant variability between the ROSAT observations obtained in 1990 and the XMM-Newton data from 2009 (c.f. Table 2). Similar to the ROSAT PSPC light curves (c.f. fig. 1 of Boller et al. 2009) no significant short timescale variability is detected within the XMM-Newton observations.

In Fig. 1 we show the power law fit to the XMM-Newton and ROSAT data. The range of photon indices listed in Table 2 belong to the steepest values obtained from quasar X-ray spectra. For comparison we list below the mean photon index plus the corresponding errors for samples of other quasars reported in the literature. For the sample of luminous SDSS quasars of Just et al. (2007) the corresponding value is $1.92^{+0.09}_{-0.08}$. The values obtained from Chandra observations of SDSS quasars by

TABLE 2
 $\Delta\chi^2 = 2.71$ CONFIDENCE LEVELS OF THE POWER LAW FIT
PARAMETERS OBTAINED FROM XMM-NEWTON AND ROSAT. THE
ROSAT AND XMM-NEWTON SPECTRA HAVE BEEN FITTED
SIMULTANEOUSLY, BUT ALLOWING THE PARAMETERS TO VARY,
GIVEN THE LARGE TIME DIFFERENCE BETWEEN THE OBSERVATIONS.
THE N_H VALUE IS FIXED TO THE VALUE OBTAINED FROM THE
ROSAT DATA DUE TO THE LOWER ENERGY COVERAGE OF ROSAT
COMPARED TO XMM-NEWTON. THE NORMALIZATION IS GIVEN IN
UNITS OF $\text{photons cm}^{-2} \text{ s}^{-1} \text{ keV}^{-1}$ AT 1 KEV.

Instrument	Photon index	norm [10^{-5}]	N_H [10^{20} cm^{-2}]
pn	3.86-4.20	2.59-3.37	2.85
M1	3.49-4.02	3.12-4.42	
M2	3.35-3.85	2.90-4.08	
ROSAT	3.92-4.41	1.08-3.28	

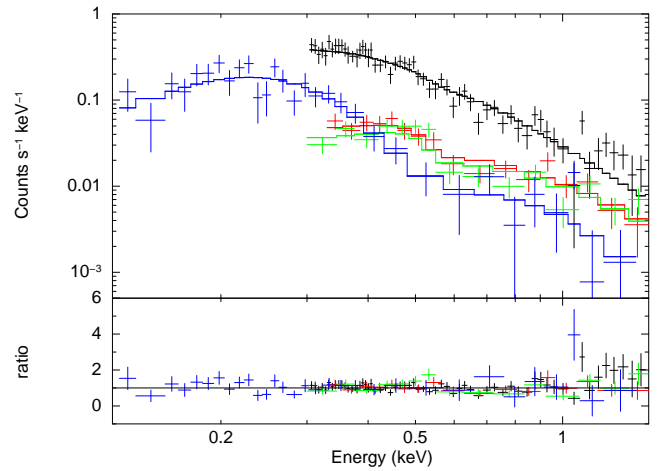


FIG. 1.— Joint fit to the ROSAT and XMM-Newton EPIC pn, MOS1, MOS2 spectra. A simple power law model with neutral absorption has been applied. All parameters are free in the fit, except the neutral absorption, which was obtained from the ROSAT observations and which gives the most precise value due to its low energy coverage. The color coding is as follows: ROSAT PSPC (blue), EPIC pn (black), MOS1 (red), and MOS2 (green).

Green et al. (2009) and on high redshift quasars by Vignali et al. (2003) are 1.94 ± 0.02 , and $1.84^{+0.31}_{-0.30}$, respectively. The mean photon index and the related errors for the highest redshift SDSS quasars obtained by Shemmer et al. (2006) is $1.95^{+0.30}_{-0.26}$. To our knowledge there are only a few other quasars with photon indices as steep as LBQS 0102-2713. Grupe et al. (1995) report on an extreme steep power law slope of about 7 in WPV007. The object is also of general interest due to the extreme X-ray variability which is most likely due to changes in the BAL flow as a result of absorption (e.g. Leighly et al. 2006).

Another example is the photon index of 4.2 derived by Komossa et al. (2000) for the NLS1 galaxy RX J0134.3-4258. Molthagen (1998) reports on a photon index of about 4.3 in RXJ0947.0+4721, and George et al. (2000) obtained a photon index of $4.18^{+0.82}_{-1.1}$ in PG 0003+199.

3.2. α_{ox} determination

The 2 keV rest-frame flux density is determined following Hogg (2000) and Weedmans's Quasar Astronomy (1986). For a photon index not equal to 2 the rest frame 2 keV flux density is given by $f_{2\text{keV}} = f(0.5 -$

$2.0) \times ((1 + \alpha_x)/(1 + z)^{\alpha_x})) \times ((\nu_{2\text{keV}}^{\alpha_x}/(\nu_{0.5\text{keV}}^{\alpha_x+1} - \nu_{0.5\text{keV}}^{\alpha_x+1})))$. The unabsorbed flux in the 0.5–2.0 keV energy band is $(1.04 \pm 0.06) \times 10^{-13}$ for MOS1, $(9.21 \pm 0.53) \times 10^{-14}$ for MOS2, $(8.82 \pm 0.07) \times 10^{-14}$ for pn, and $(6.73 \pm 0.41) \times 10^{-14}$ erg cm $^{-2}$ s $^{-1}$ for ROSAT. Using the full range of unabsorbed 0.5–2.0 keV flux measurements and the photon indices listed in Table 2, one obtains a 2 keV flux density that ranges between $(8.83 \pm 0.52) \times 10^{-32}$ and $(2.05 \pm 0.12) \times 10^{-31}$ erg cm $^{-2}$ s $^{-1}$ Hz $^{-1}$. From the Swift UVOT data we derive an extinction corrected flux at 2500 Å rest frame wavelength of $(6.35 \pm 0.02) \times 10^{-27}$ erg cm $^{-2}$ s $^{-1}$ Hz $^{-1}$. The corresponding α_{ox} values range between (-1.87 ± 0.11) and (-2.11 ± 0.12) , respectively. These values are somewhat lower compared to the -2.2 value obtained from the ROSAT data in Boller et al. (2009) due to the steeper photon index assumed of 6. The range in the α_{ox} values obtained from the additional first XMM-Newton and Swift observations provide more precise measurements.

Just et al. (2007) argued that α_{ox} decreases with increasing 2500 Å luminosity density. In their fig. 7 the α_{ox} values range between about -1.0 and -2.2, and the log $L_{2500\text{\AA}} = l_{\text{UV}}$ luminosity density ranges between about 27.8 and 32.5. LBQS 0102-2713 exhibits a luminosity density at 2500 Å of $L_{2500\text{\AA}} = (5.67 \pm 0.02) \times 10^{31}$ erg s $^{-1}$ Hz $^{-1}$ corresponding to a value of $l_{\text{UV}} = (31.75 \pm 0.001)$. Therefore the source is located at the higher end of the l_{UV} distribution. The α_{ox} values given above on the other hand are at the lower end compared Just et al. (2007). The corresponding $\Delta\alpha_{\text{ox}}$ values are ranging between -0.05 and -0.5. All this is further supporting the trend whereby α_{ox} decreases with increasing UV luminosity density.

4. SED SPECTRAL FITTING

We have fitted the Swift UVOT, XMM-Newton and ROSAT data with an accretion disc spectrum *diskpn* and the *compTT* model including absorption by neutral hydrogen *TBabs* and the corresponding extinction value *red den*. As absorption above the Galactic value is required, the N_{H} value is allowed to vary to obtain the best value for the total luminosity. The $\Delta\chi^2 = 2.71$ confidence levels range between $(2.3 \text{ and } 3.9) \times 10^{20}$ cm $^{-2}$, slightly above the values derived from the ROSAT power law fit. The X-ray absorption by the ISM is accounted for by the *XSPEC* model *TBabs* (Wilms et al. 2000). The *red den* model describes the infrared, optical, and ultraviolet extinction (Cardelli et al. 1989). The *diskpn* model available within *XSPEC* is an extension of the *diskbb* model of Mitsuda et al. (1984) and Makishima et al. (1986) and describes the black body emission of a disk in the pseudo-Newtonian potential (for details see Gierlinski et al. 1999). A part of the thermal disc photons are Comptonized in a hot plasma described by the *compTT* model Titarchuk (1994). Both models components are available within the version of *XSPEC* that we used. The phenomenological model gives an acceptable fit to the Swift UVOT, XMM-Newton and ROSAT data. The temperature of the *diskpn* model is 30 ± 4 eV. The inner radius is fixed to 10 R_{G} and the normalization is 171 ± 5 . The normalization is given in units of $(M^2 \cos i)/(D^2 \beta^4)$. The input soft photon temperature of the *compTT* model is fixed to the temperature of the *diskpn* spectrum and

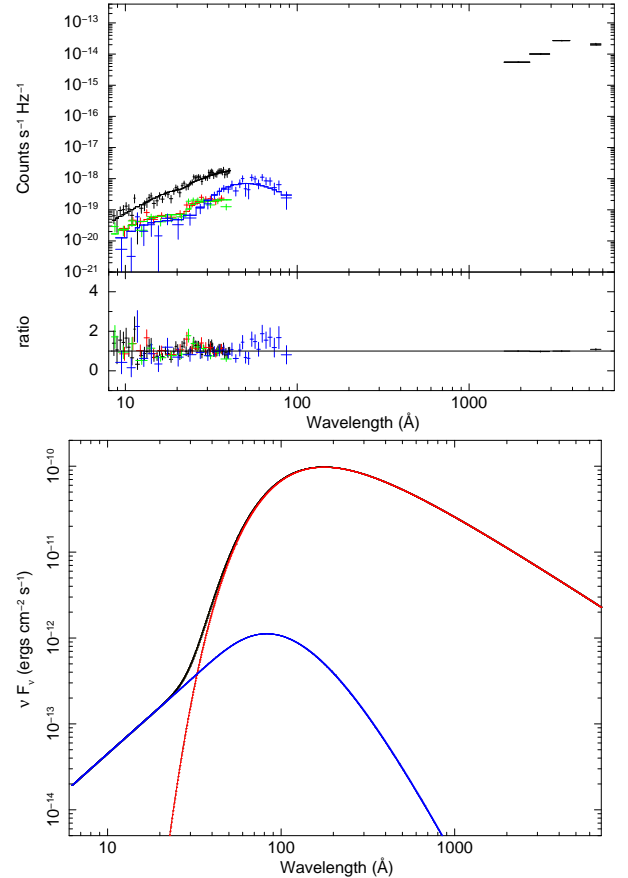


FIG. 2.— Upper panel: Fit to the Swift UVOT, XMM-Newton and ROSAT data for an accretion disc spectrum which is partially Comptonized. The UVOT data describe the emission from the accretion disc and the soft X-ray flux is arising due to Comptonization of parts of the accretion disc by a hot electron layer. Lower panel: The unfolded model spectrum. Note the strong UV luminosity and the X-ray luminosity close to 2 keV, which differ by about 4 orders of magnitude in the νf_ν parameter space.

the normalization is $(1.80 \pm 0.21) \times 10^{-4}$. As the high energy cut-off is not detected in the data, the electron temperature has been fixed to 50 keV. The plasma optical depth is $(4.20 \pm 0.69) \times 10^{-2}$ which is a lower limit given the fact the the high energy cut-off is not detected. The reduced χ^2 value is 1.09 for 114 d.o.f.

The unabsorbed luminosity derived from the spectral fit is 6.20×10^{47} erg s $^{-1}$ in the energy range between 0.001 and 2 keV. Using the two extreme normalization values for each relevant model component we derive a lower value and upper value for the unabsorbed luminosity of 6.01×10^{47} erg s $^{-1}$ and 6.42×10^{47} erg s $^{-1}$. We note that the luminosity is comparable to the mean value of the most luminous quasars obtained by Richards et al. (2006). Assuming an Eddington ratio of 1, this translates to a lower limit of the black hole mass of $(4.50^{+0.15}_{-0.17}) \times 10^9 M_{\odot}$, which would appear on the upper mass scale for black holes. However, as it is known for the lower luminosity NLS1 analogues, the Eddington ratio might exceed 1 for objects with steep soft X-ray photon indices and narrow optical line widths.

A more reliable mass and Eddington ratio estimation can be obtained using the Mg II rest frame line width which is 2200 km s $^{-1}$ (Boller et al. 2009) and the optical observation obtained by Morris et al. (1991). Following equ. 10

of Wang et al. (2009), the Mg II FWHM line width and the λL_{λ} 3000 Å value of $3.2 \times 10^{45} \text{ erg s}^{-1}$ translate into a black hole mass of $(2.51^{+4.34}_{-1.60}) \times 10^8 M_{\odot}$ assuming a luminosity distance of $D_L = 1.5 \times 10^{28} \text{ cm}$. The corresponding Eddington luminosity is $(3.46^{+5.99}_{-2.20}) \times 10^{46} \text{ erg s}^{-1}$. Taking into account the lower and upper values for the unabsorbed luminosity and the Eddington luminosity, respectively, the Eddington ratio is $L/L_{\text{edd}} = 17.92^{+33.0}_{-11.5}$. Eddington ratios have been estimated by several authors. Onken and Kollmeier (2008) found Eddington ratios for SDSS quasars ranging between 0.01 and 1. Shemmer et al. (2004) derive values for the Eddington ratio ranging between 0.14 and 1.71 (their Table 2). We note that LBQS 0102-2713 appears to exhibit one of the highest Eddington ratios measured from accreting black holes so far.

5. SUMMARY

The NLS1 quasar LBQS 0102-2713 exhibits an unusual parameter combination derived from archival ROSAT and the first XMM-Newton and Swift observations that can be summarized as follows: (i) the soft X-ray photon index ranges between 3.35 and 4.41 and belongs to the steepest values observed so far; (ii) the α_{ox} value ranges between (-1.87 ± 0.11) and (-2.21 ± 0.12) , similar to the highest values observed in BAL quasars (c.f. table 3 of Gallagher et al. 2006); (iii) in contrast to BAL quasars, LBQS 0102-2713 is not significantly absorbed, the most precise measurement, which comes from ROSAT observations, is $2.85 \times 10^{20} \text{ cm}^{-2}$, at least two orders of magnitude lower compared to BAL quasars; (iv) the 2 keV monochromatic luminosity is comparable to the mean value for quasar SED's, however the object is not intrinsically X-ray weak, in contrast to PHL 1811 which shows similar observational properties; (v) the UV-X-ray luminosity is $6.20^{+0.22}_{-0.19} \times 10^{47} \text{ erg s}^{-1}$, about two orders of magnitude above the mean of quasar SED's, and the ratio of the UV peak to 2 keV X-ray luminosity is about 10^4 in the νF_{ν} space; (vi) the Eddington ratio appears extremely high with $L/L_{\text{edd}} = 17.92^{+33.0}_{-11.5}$ compared to other quasars studies. (vii) no X-ray emission is detected above 2 keV and the upper limit obtained from the first XMM-Newton observations is $2 \times 10^{-14} \text{ erg cm}^{-2} \text{ s}^{-1}$.

6. DISCUSSION

We have fitted the Swift UVOT, XMM-Newton and the ROSAT data with an accretion disc spectrum in the pseudo-Newton potential. The temperature of the seed photons is $T_{\text{seed,max}} = (30 \pm 4) \text{ eV}$. A part of the thermal disc photons are comptonized in a plasma cloud with some Thomson depth $\tau_{\text{electrons}}$ and a temperature $T_{\text{electrons}}$. The mean change in photon frequency is given by $\Delta\nu/\nu = (4kT_e - h\nu)/m_e c^2$ (Titarchuk and Hua 1997). For a thermal distribution of electrons the dimension-

less electron temperature is $\theta = kT_e/m_e c^2$. The scattered input and output photon energies are related by $\epsilon_{\text{out,N}} = (1 + 4\theta)^N \epsilon_{\text{in}} = 3\theta$, where N is the number of scattering events which depend on the plasma optical depth. The shape of the spectrum is determined by the Comptonization parameter $y = kT_e/m_e c^2 N$ (Titarchuk and Hua 1997). The relation between the photon index and the electron temperature is $\Gamma = (\ln\tau)/\ln(1 + \theta)$. For a given optical depth a steep power law means that the electron temperature is low. The comptonized UV seed photons give rise to the observed X-rays as detected with ROSAT and XMM-Newton. With this model we are able for the first time to explain the UV and X-ray emission. As no thermal energy cut-off is detected in the Comptonized spectrum, the plasma optical depth $\tau_{\text{electrons}}$ and the electron temperature $T_{\text{electrons}}$ cannot be reliably determined from the *compTT* model. However the Comptonization parameter y can be derived from the power law spectrum. The $\Delta\chi^2 = 2.71$ confidence levels for the photon indices listed in Table 1 translate to y values ranging between 4.5×10^{-2} and 7.9×10^{-2} .

As the thermal cut-off is not detected, only some estimates on the temperature of the plasma can be made. We note that the source is accreting above the Eddington limit and that in such cases outflowing winds are expected with some significant optical depth. Following Rybicky and Lightman (1979) the relation between the Comptonization parameter, the dimensionless electron temperature and the plasma optical depth is $y = 4\theta \times \tau_{\text{electrons}}$. Assuming a plasma optical depth ≥ 1 , an upper limit for θ can be derived. Using the y values given above and $\tau_{\text{electrons}} = 1$ the upper-limit on θ ranges between 1.1×10^{-2} and 2.0×10^{-2} , corresponding to electron temperatures ranging between 5.6 and 10.2 keV. To check that this is consistent with our spectral data, we fixed the plasma optical depth to $\tau_{\text{electrons}} = 1$ in the spectral fit described in Section 4, and we derived an electron temperature of $(6.8 \pm 0.4) \text{ keV}$, in agreement with the analytical calculations. Longer X-ray observations are required to finally detect the thermal cut-off and to precisely determine the coronal parameters.

The authors would like to thank the anonymous referee for her/his detailed and extremely helpful report. TB is grateful for critical reading of the paper by A. Müller and M. Gilfanov as well as constructive discussions with S. Nayakshin. TB especially thanks C. Done for fruitful discussions on the SED spectral fitting of the source and the importance of Comptonization to explain the X-ray emission in super-Eddington sources. TB thanks S. Immler for the discussions on the importance of the Swift satellite for observing UV bright distant AGNs.

Facilities: ROSAT, HST FOS, XMM-Newton, Swift.

REFERENCES

- Arnaud K. A., 1996, in Jacoby G., Barnes J., eds, ASP Conf. Ser. Vol. 101, Astronomical Data Analysis Software and Systems V. Astron. Soc. Pac., San Francisco, p. 17
- Boller Th., Linguri K., Heftrich T., Weigand M., ApJ 699, 732, 2009
- Brotherton, M. S.; Arav, Nahum; Becker, R. H.; Tran, Hien D.; Gregg, Michael D.; White, R. L.; Laurent-Muehleisen, S. A.; Hack, Warren, ApJ, 546, 134, 2001
- Arnaud K. A., 1996, in Jacoby G., Barnes J., eds, ASP Conf. Ser. Vol. 101, Astronomical Data Analysis Software and Systems V. Astron. Soc. Pac., San Francisco, p. 17
- Cardelli, J.A., Clayton, G.C., Mathis, J.S., ApJ 345, 245, 1989

- Dickey, J.M., Lockman, F.J., ARA&A 28, 215, 1990
- Gallagher, S. C., Brandt, W. N., Chartas, G., Priddey, R., Garmire, G. P., Sambruna, R. M., ApJ, 644, 709, 2006
- George, I. M., Turner, T. J., Yaqoob, T., Netzer, H., Laor, A., Mushotzky, R. F., Nandra, K., Takahashi, T., ApJ, 531, 52, 2000
- Gibson, R.R., Brandt, W.N., Schneider, D.P. 2008, ApJ, 685, 773
- Gierlinski, M., Zdziarski, A., Poutanen, J. et al., MNRAS, 309, 496, 1999
- Green, P.J., Aldcroft, T.L., Richards, G.T., Barkhouse, W.A., Constantin, A., Haggard, D., Karovska, M., Kim, D.-W., Kim, M., Vikhlinin, A., Anderson, S. F., Mossman, A., Kashyap, V., Myers, A.C., Silverman, J.D., Wilkes, B.J., Tananbaum, H., ApJ 690, 644, 2009
- Grupe, D., Beuerman, K., Mannheim, K., Thomas, H.-C., Fink, H. H., de Martino, D., A&A 300, 21, 1995
- Hewett, P.C., Foltz, C.B., Chaffee, F.H., AJ 109, 1498, 1995
- Hogg, David W.; astro-ph/9905116, 2000
- Just, D. W., Brandt, W. N., Shemmer, O., Steffen, A. T., Schneider, D. P., Chartas, G., Garmire G. P., ApJ 665, 1004, 2007
- Kaspi, S., Smith, P. S., Netzer, H., Maoz, D., Jannuzi, B. T., Giveon, U. ApJ 533, 631, 2000
- Komossa, S., Breitschwerdt, D., Greiner, J., Meerschweinchen, J., Ap&SS 272, 303, 2000
- Leighly, K., Casebeer, D., Hamann, F., Grupe, D., Bulletin of the American Astronomical Society, Vol. 38, 355, 2006
- Leighly, Karen M.; Halpern, Jules P.; Jenkins, Edward B.; Casebeer, Darrin, ApJS, 173, 1, 2007
- Makishima, K., Maejima, Y., Mitsuda, K. et al. ApJ 308, 635, 1986
- Mitsuda, K., Inoue, H., Koyama, K., Makishima, K., Matsuoka, M., Ogawara, Y., Suzuki, K., et al., PASJ, 36, 741, 1984
- Molthagen K., Bade N., Wendker H. J., A&A 331, 925, 1998
- Morris, S.L., Weymann, R.J., Anderson, S.F., et al., AJ 102, 1627, 1991
- Osterbrock, D. E., Pogge, R. W., ApJ, 297, 166, 1985
- Richards, G., Lacy, M., Storrie-Lombardi, L., Fan, X., Papovich, C., Gallagher, S., Hall, P., Hines, D., Anderson, S., Jester, S., Schneider, D., Vanden Berk, D., Strauss, M., York, D., ApJS, 357, 261, 2006
- Rybicki, G. B., Lightman, A. P., ASTRONOMY QUARTERLY V. 3, P. 199, Book-Review - Radiative Processes in Astrophysics, 1980
- Shemmer O., Netzer H., Maiolino R., Oliva E., Croom S., Corbett E., di Fabrizio L., ApJ 614, Issue 2, 547, 2004
- Shemmer O., Brandt W. N., Schneider D. P.; Fan X., Strauss M. A., Diamond-Stanic A. M., Richards, G. T., Anderson S. F., Gunn, J. E., Brinkmann J., ApJ 644, 86, 2006
- Titarchuk, L.G., ApJ 434, 570, 1994
- Titarchuk, L.G., Xin-Min Hua, X.M., Adv. Space Res. Vol 19, No. 1, 99, 1997
- Trümper J. E.; Hasinger G., The Universe in X-Rays edited by Joachim E. Trümper and Günther Hasinger. Extraterrestrial Physics & Space Sciences. Springer, 2008.
- Onken, Christopher A.; Kollmeier, Juna A., ApJ 689, 130, 2008
- Titarchuk L., ApJ 434, 570, 1994
- Vanden Berk, Daniel E.; Richards, Gordon T.; Bauer, Amanda; Strauss, Michael A.; Schneider, and 60 coauthors, AJ, 122, 549, 2001
- Vignali, C., Brandt, W.N., & Schneider, D.P., AJ, 125, 433, 2003
- Wang Jian-Guo, Dong Xiao-Bo, Wang Ting-Gui, Ho, Luis C., Yuan Weimin, Wang Huiyuan, Zhang Kai, Zhang Shaohua, Zhou Hongyan, ApJ 707, 1334, 2009
- Weedman, Daniel W., Quasar astronomy, 1986qa, book, 1986
- Wilms, J., Allen, A., McCray, R., ApJ 542, 914, 2000
- Zheng, Wei; Kriss, Gerard A.; Telfer, Randal C.; Grimes, John P.; Davidsen, Arthur F., ApJ, 475, 469, 1997